

UNCLASSIFIED

AD 274 156

*Reproduced
by the*

ARMED SERVICES TECHNICAL INFORMATION AGENCY
ARLINGTON HALL STATION
ARLINGTON 12, VIRGINIA



UNCLASSIFIED

NOTICE: When government or other drawings, specifications or other data are used for any purpose other than in connection with a definitely related government procurement operation, the U. S. Government thereby incurs no responsibility, nor any obligation whatsoever; and the fact that the Government may have formulated, furnished, or in any way supplied the said drawings, specifications, or other data is not to be regarded by implication or otherwise as in any manner licensing the holder or any other person or corporation, or conveying any rights or permission to manufacture, use or sell any patented invention that may in any way be related thereto.

274 156

274 156

SECTION T

THE JOHNS HOPKINS UNIVERSITY
APPLIED PHYSICS LABORATORY
8621 Georgia Avenue, Silver Spring, Maryland

CM-1002

Operating under Contract NOrd 7386 with the
Bureau of Naval Weapons, Department of the Navy

Copy No. 12

A PROPOSED ULTRASONIC
ACQUISITION SYSTEM
FOR
PULSED RADAR

Released to ASTIA by the
Bureau of
without restriction.

by

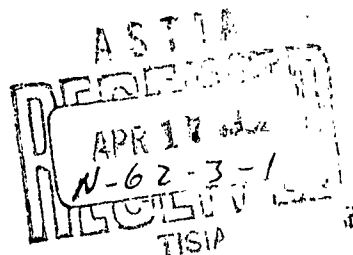
T. Calhoon

A. Finkel

J. Kuck

W. Liben

NAVAL WEAPONS



September 1961

CM-1002
September 1961

A Proposed Ultrasonic Acquisition System for Pulsed Radar

by
**T. Calhoon
A. Finkel
J. Kuck
W. Liben**



**THE JOHNS HOPKINS UNIVERSITY
APPLIED PHYSICS LABORATORY**
8621 GEORGIA AVENUE SILVER SPRING, MARYLAND

TABLE OF CONTENTS

List of Illustrations	iii
I. INTRODUCTION	1
II. DESCRIPTION OF SYSTEM	2
Storage Tube Equipment	9
Storage Tube Sweep Generators	12
Storage Tube Unblanking	20
Target Switching	21
Storage Tube Input Amplified	23
Storage Tube Output Amplifier	24
Storage Tube Performance	24
Master Timing and Mode Switching Unit	27
Ultrasonic Cell	30
Light Source	33
Optics and Photometry	33
ULM Cell Driving Amplifier	38
Image Converter	39
III. ACQUISITION SYSTEM PERFORMANCE	41

LIST OF ILLUSTRATIONS

<u>Figure</u>		<u>Page</u>
1	Bipolar Sampling of Doppler Frequency . . .	2
2	Single Analyzer Channel Acquisition System . . .	3
3	Multiple Target Returns on Storage Tube . . .	5
4	Range Velocity Display	9
5	Circuits for WL 7225 Storage Tube (Mod B) Block Diagram	11
6	Sweep Generator Chassis for WL 7225 Storage Tube	14
7	Sweep Generator Output in the Read Mode . . .	16
8	Deviation of Sweep Voltage from Arbitrarily Chosen Linear Sweep (H-Write Positive Going) (H-Write Negative Going)	17
9	Deviation of Sweep Voltage from Arbitrarily Chosen Linear Sweep (H-Read Positive Going) (H-Read Negative Going)	18
10	Expanded View of a Portion of the Vertical Read Outputs	19
11	Target Switching and Gating Operation, Block Diagram	23
12	Output of Time-Compressed Doppler Filter and Detector Circuit During the Read Frame Interval (Target Signal from Simulator)	26
13	Block Diagram Showing System Timing Interconnections	28

<u>Figure</u>		<u>Page</u>
14	Ultrasonic Light Modulator	31
15	Spectral Components of a Train of Square Pulses -- Analysis by Ultrasonic Cell	34
16	14.75 mc Ultrasonic Light Modulator Making Spectrum Analysis of Random Bipolar Video Pulses	35
17	Optical System Used with Ultrasonic Cell, Image Converter, and Image Orthicon	36
18	Prototype Acquisition System	42
19	Range-Doppler Display With and Without Adding Jamming Noise	43

A PROPOSED ULTRASONIC ACQUISITION SYSTEM FOR PULSED RADAR

I. INTRODUCTION

The system described in this paper was designed and constructed to test techniques for a radar acquisition system capable of high speed data processing. A description of a system instrumented to measure range to 100 feet and doppler shift to 300 cps is given in this paper.

The range and doppler resolutions referred to above should not be construed to be the ultimate; they were selected for convenience rather than to illustrate the ultimate.

II. DESCRIPTION OF SYSTEM

The acquisition system was designed as a frequency analyzer of random timed bipolar video pulses generated as follows: A radar transmitter transmits a randomly timed r-f pulse in a selected direction. If the pulse is returned from a target, it is mixed with the transmitted frequency. Since the reflected pulse is shifted in frequency by the target doppler shift, the result of the mixing is a d-c pulse which is a sample of a wave equal in frequency to the doppler shift. The width of the bipolar video pulse equals the original r-f pulse width. The origin of these bipolar pulses is shown in Fig. 1.

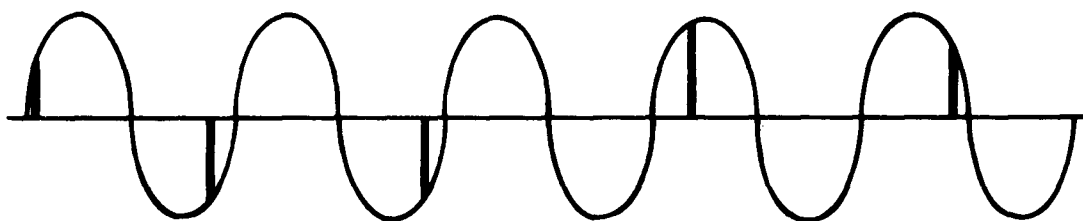


Fig. 1 BIPOLAR SAMPLING OF DOPPLER FREQUENCY

The input to the acquisition system is, therefore, a stream of bipolar video pulses of varying height and spacing.

A simplified block diagram for an analyzer for one frequency is shown in Fig. 2. Such a system was constructed to illustrate the feasibility of the analyzer. The parameters

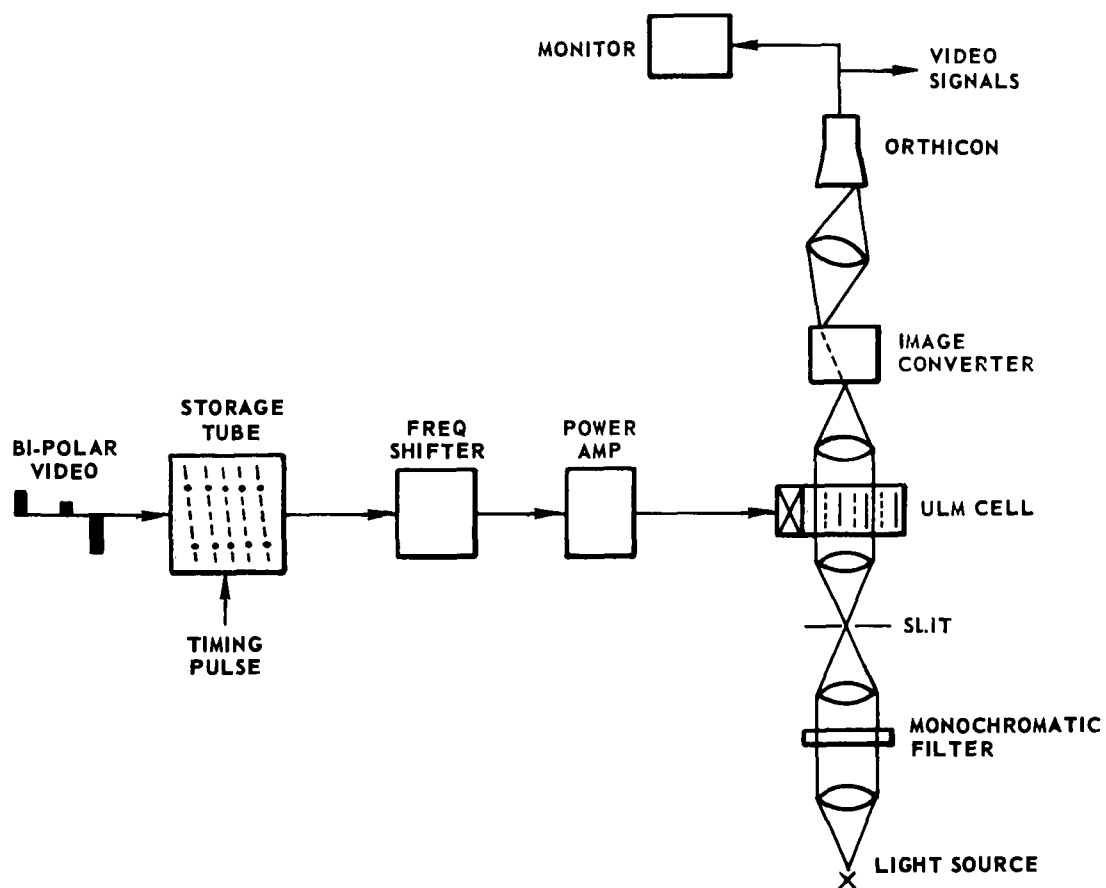


Fig. 2 SINGLE ANALYZER CHANNEL ACQUISITION SYSTEM

selected were as follows: average pulse repetition of 16,667 pulses/second; pulse transmission time was random within a 5 microsecond period which occurred at 20 microsecond intervals; doppler bandwidth to be 2-8 kc; range resolution to be 100 feet; doppler resolution to 1/20; total range increment to be 5000 feet.

The acquisition system channel can be broken down into four major subdivisions: (1) the storage tube and its associated electronics; (2) a master timer used to time all the operations of the system; (3) the Ultrasonic Light Modulator (ULM) with its associated crystal driving amplifier and optical system; and (4) the image converter and image orthicon read-out system.

Wherever, in this description, an operation is described which requires precise timing, it is to be understood that the timing was accomplished by a timing pulse from the master timer. Only rarely will the timer be specifically mentioned.

When a pulse is transmitted and a return received and mixed with the transmitted pulse, the resulting bipolar video pulse is applied to the storage tube "write" grid. If it is desired to examine an increment in range from R_0 to $R_0 + \Delta R$, the trigger is delayed by a programmer by an amount equal to twice the travel time to R_0 . The $2R_0$ delayed timing pulse starts a vertical sweep of the storage tube "write" gun. If a target is located with ΔR , the bipolar pulse is written in at a point on the storage tube

corresponding to the target position. If there are two targets in ΔR , two bipolar pulses will be written as shown in Fig. 3. Since the range increment is to be 5000

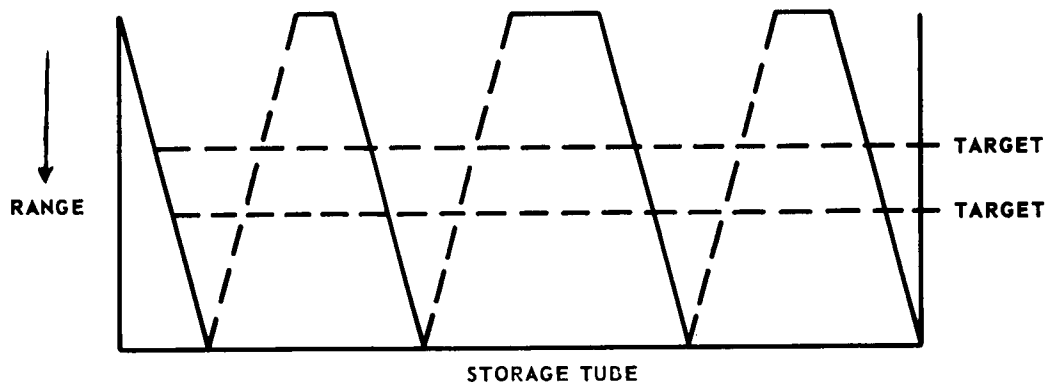


Fig. 3 MULTIPLE TARGET RETURNS ON STORAGE TUBE

feet with a resolution of 100 feet, there will be 50 range elements of 0.2 microsecond each, making a storage tube vertical "write" time of 10 microseconds. Meanwhile, the horizontal "write" sweep has been initiated by the programmer at time zero. Since the doppler resolution is to be $(8000-2000)/20 = 300$ cps, the information gathering time is $1/300$ second. When the 10 microsecond vertical "write" period is completed, the beam returns to the top and continues to move horizontally until the next randomly timed pulse is transmitted; whereupon, the entire cycle is

repeated as before. From the list of parameters we see that the shortest time between two successive pulses is 35 microseconds. Since the vertical "write" time is 10 microseconds and the flyback time is just under 10 microseconds, there will be some waiting time at the top before the next vertical "write" operation is started. During the second vertical "write" operation, bipolar pulses will again be written as before and at the same horizontal level or range element. Since a doppler frequency of 8000 cps at X-band corresponds to approximately 400 ft/sec target radial speed, and total "write-in" time is 1/300 second, the spread in range of all target returns will be 1.3 feet.

Since the average pulse rate is 50 kcps/3 and the total "write" time is 1/300 second, $50 \times 10^3 / (3 \times 300) = 56$ bipolar video returns will be written in at the appropriate range element for each target. In Fig. 3 we show only four.

The bipolar video pulses stored in the storage tube are now read out, one range element at a time, by making a horizontal sweep across the tube, return and vertical step of one range element, and repeat of horizontal "read-out." In this way for each range element we read out, either tube noise alone if a target is not located in that range element, or tube noise plus bipolar video pulse if a target is located in that range element.

The time used in reading out each range element is fixed by the desired doppler bandwidth which the spectrum analyzer can handle. If the "read-out" is faster than the "write-in," then the doppler frequency is multiplied by the ratio of these two speeds. In our case we wish to increase the doppler frequency by a factor of 100, so the "read-out" time is $1/100 \times 1/300 = 33$ microseconds.

Thus, the storage tube accomplishes the following: it rearranges the radar returns, grouping them by target; it raises the doppler frequency to a useful value; and it provides range gating.

The output of each range element is now mixed with a carrier frequency in a balanced modulator. This is required since the ultrasonic spectrum analyzer is driven by a quartz crystal with a Q of 12 at a convenient carrier frequency; in our case this is 20 mc. The output of the balanced modulator consists of the carrier plus the two sidebands. The carrier is present since the storage tube "write" grid is operated at a bias point of -20 volts to allow "write-in" of both polarities of the bipolar video pulses. On "read-out" the pulses are of one polarity only so that the input to the modulator is not balanced and the carrier appears along with the sidebands.

The signal is amplified and applied to the piezo crystal driving the fluid in the ultrasonic spectrum analyzer. Any frequency component present in the signal to the quartz piezo crystal will produce a light beam whose position is a function of the frequency of the signal and whose intensity depends upon the amplitude of the component.

The image plane of the spectrum analyzer now has three lines of light corresponding to the carrier and the two sidebands. The image, or optical signal, is focused on the

photocathode of an image converter tube. An image converter is made up of three elements: a photocathode which emits electrons from each point in proportion to the light intensity incident at that point; an electron lens which focuses the electrons upon a fluorescent screen; and a fluorescent screen upon which the focused electrons produce an optical image corresponding to the image focused on the cathode. The converter selected possesses two useful properties: the electron beam emitted by the photocathode can be gated on or off by a grid placed close to the cathode; and the image can be deflected across the phosphor by applying a voltage to a pair of deflecting plates in the converter.

During operation the gating grid is biased off except when all the signals from one range element on the storage tube are in the ultrasonic cell. The converter is then gated on for a short time so that the image on the converter screen is sharpened by not using the signal except when all the available information is stored in the ultrasonic cell.

Since the image produced by a single range element consists of three spots of light in a row and successive range elements would produce noise outputs at the same location, it is necessary to separate the outputs from the successive range elements. This is done by deflecting the outputs from successive range elements to parallel contiguous lines. In this way a range scale is built up in the deflection direction, which is normal to direction of the doppler scale. Thus, a range-doppler display is constructed, Fig. 4.

The converter output is focused onto an image orthicon which will read out the range elements individually and in succession. The presence of a target on a range element would be indicated by a pulse in the video output of the image orthicon.

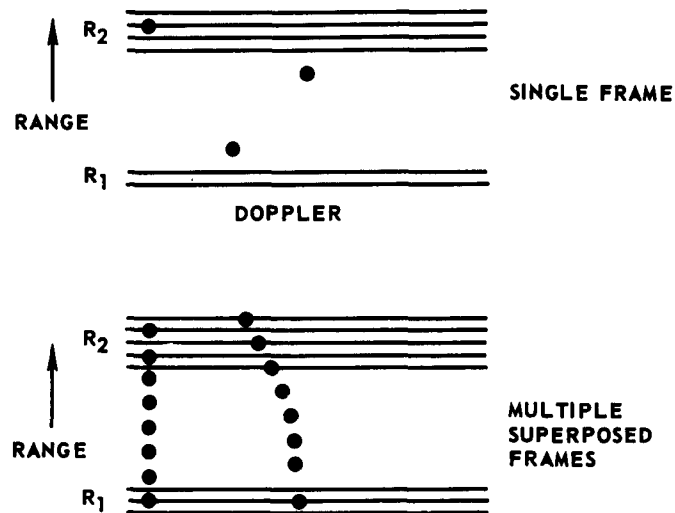


Fig. 4 RANGE VELOCITY DISPLAY

In the system actually instrumented, the image orthicon read out was omitted since it was not required to demonstrate the basic analyzer performance. But enough information was made, available to conclude that with the presently produced type 5820 image orthicon tubes, the performance would have been submarginal. This poor performance is caused, to a great extent, by the decreasing resolution of the image orthicon as the illumination level decreases.

Storage Tube Equipment

The system requires a storage tube with associated input and output amplifiers, deflection circuits, mode switching circuits and power supplies.

The storage tube is the Westinghouse type WL7225 barrier grid storage tube (the "Radechon"). This is an electrical

input-electrical output tube. The tube erases during the reading operation so that the tube is used for only a single "read-out" of the stored information. The degree of erasure and the amplitude of the read-out signal achieved during a single "read-out" varies depending on the sweep speed and beam current (which is controlled by the grid bias).

Figure 5 is a block diagram showing the storage equipment and the master timer. This equipment fills two racks.

There is not enough space here to go into all of the details of the storage tube circuitry, but a few items, which involved unusual design problems will be mentioned briefly. Those who may be interested in studying the circuit details are referred to the Applied Physics Laboratory report on the Acquisition System (APL/JHU CF-2904).

The sweep circuits which furnished deflection voltage to the storage tube constituted an especially difficult problem.

The specifications required that both the vertical and horizontal sweep circuit be capable of generating linear, sawtooth sweep voltages on command, i.e., on receipt of suitably timed trigger pulse. These would not necessarily occur at a uniform pulse repetition frequency. Sweep speeds for "write" and "read" were different. During "write" the vertical sweep was fast—25 microseconds for a full sweep across the raster and during "read" it was slow—8 milliseconds for a full sweep. In use 40 per cent of the usable vertical raster height was used. The horizontal sweep was three milliseconds in write and 30 microseconds in read.

The sweep amplitude required to produce a full size Square raster, the corners of which would just reach the edge of the circular storage target, was about 400 volts peak-to-peak between deflection plates.

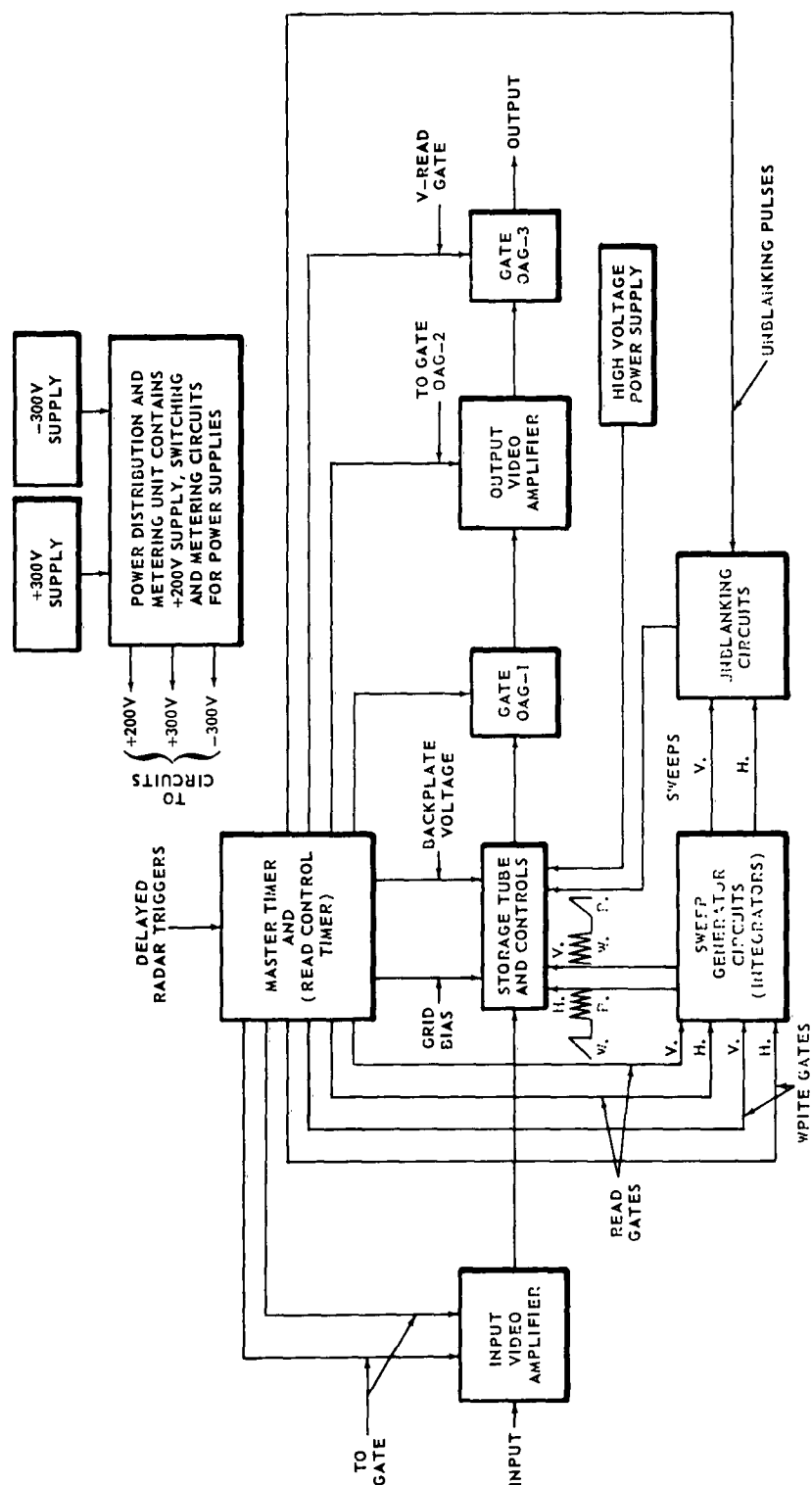


Fig. 5 CIRCUITS FOR WL 7225 STORAGE TUBE (MOD. B)
BLOCK DIAGRAM

It was desired that sweep linearity be high, at least of the order of one per cent. Higher linearity, if achieved, would be worthwhile in that it would demonstrate the feasibility of using such deflection circuits in future, more advanced systems. These systems may require linearity as high as one part in several thousand.

The vertical "write" sweep was to be triggered at variable time, the minimum time between triggers being 35 microseconds. The original goal was a sweep flyback time of less than 5 microseconds. This goal was later relaxed to 10 microseconds, but before that was done, a great deal of time and effort was expended in attempting to reach the earlier goal. Flyback times as short as 3 microseconds were observed during the experimental work. At present, the flyback times are about 6 microseconds. This is the time for the visible transients to die out, as judged visually from an oscilloscope display of the sweep voltage.

A requirement which was placed on the vertical "read" sweep during the development was that the linear saw-tooth voltage waveform be modified to a series of steps such that the voltage would remain constant during each 30 microsecond horizontal "read" sweep interval and would increase only during the 34-microsecond intervals between the horizontal read-out sweeps. This would eliminate the change in range that would otherwise occur along the horizontal read-out lines.

Storage Tube Sweep Generators

The circuit configurations for the vertical and horizontal deflection circuits were nearly identical. The different sweep speeds required were obtained by variation of the

values of two pairs of resistors in each circuit. The only requirement that prevented identical configurations was that a slight modification was required to make the vertical circuit produce the aforementioned step waveform during "read."

The basic element of the sweep generator circuit was an integrator driven by a rectangular input pulse. The integrator was built around a commercially available, wideband operational amplifier—a type which is normally used in computer applications. This amplifier was the Philbrick, Model USA-3, chopper stabilized, 4-tube d-c amplifier with a specified open loop d-c gain of ten million and unity gain at one mc. It was necessary to add a cathode follower input stage ahead of this amplifier in order to obtain higher input impedance at high frequencies. This was incorporated in such a way that the chopper stabilization was still effective in eliminating d-c drift.

It was desired to avoid the use of a deflection amplifier between the sweep generator and the deflection plates because of the distortion that might be introduced by such an amplifier. Therefore, it was decided that the sweep generator should be designed to deliver a large enough sweep voltage at the correct d-c level so that it could be coupled directly to the deflection plates of the storage tube. These deflection plates must be at an average potential of +150 volts at all times during the sweep to maintain proper focus of the storage tube. This required that an additional output stage be added onto the Philbrick amplifier inside the integrator feedback loop. In order to obtain a pushpull output to drive the deflection plates, each sweep generator channel, i.e., vertical or horizontal channel, contained two integrators sweeping in opposite directions. Figure 6 is a block diagram

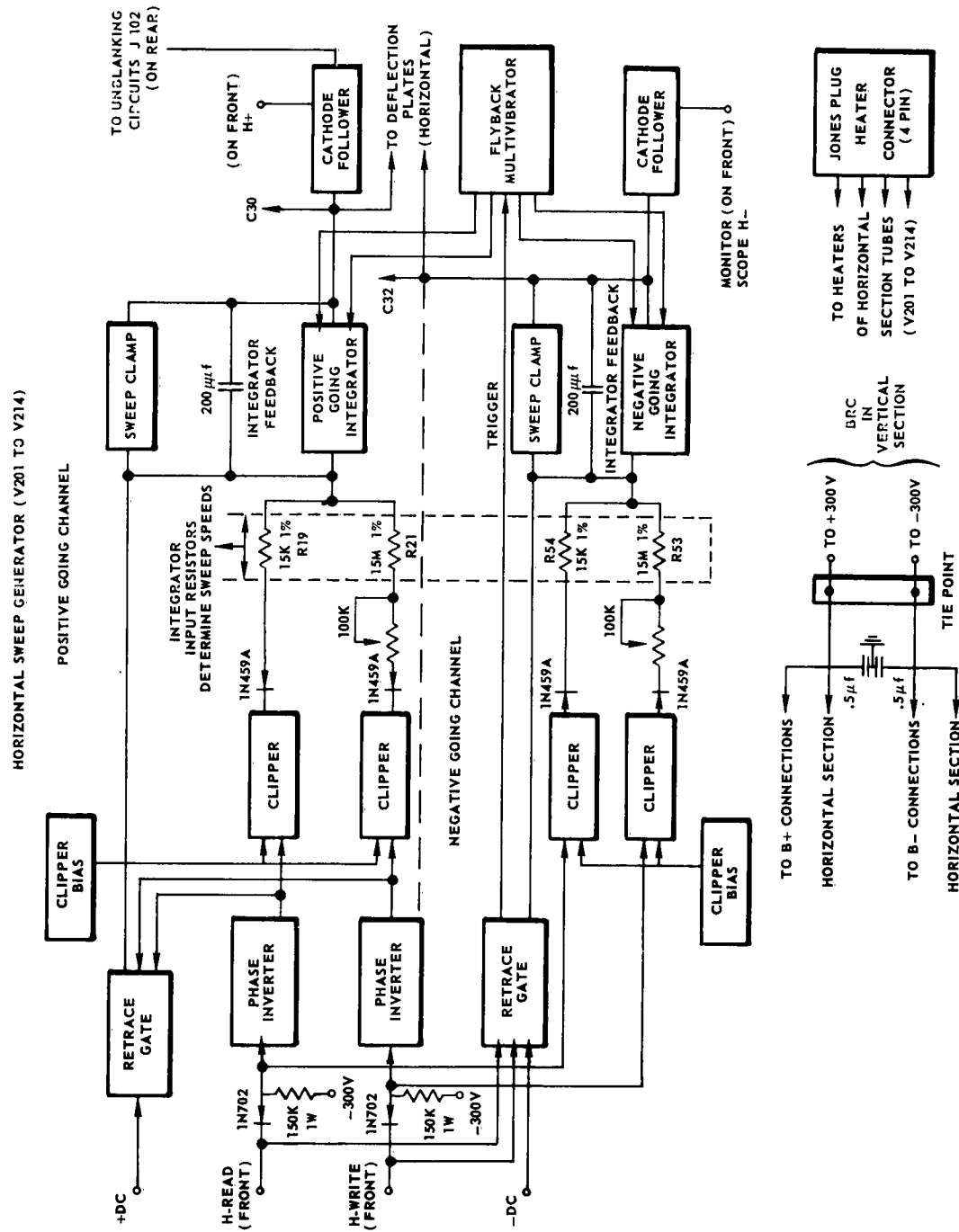


Fig. 6 SWEEP GENERATOR CHASSIS FOR WL 7225 STORAGE TUBE

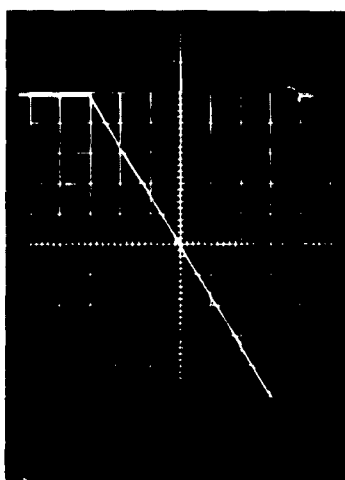
of the positive and negative going horizontal channels of the sweep generator. A similar pair of positive and negative going channels was used for the vertical sweep generator. All of these channels, were on a single chassis, which contains four Philbrick USA-3 amplifiers plus 28 tubes.

The separate generation of slow and fast sweep speeds by the same sweep integrator was accomplished by feeding separate input pulses through separate input resistors to the integrator. One pulse generator delivers a long pulse through high valued input resistors (R21 and R53) to the integrators to develop the slow sweep. The other generator delivers a short pulse through low resistances (R19 and R54) to generate the fast sweep. Either generator may be triggered at will with a random pulse repetition frequency. A diode clamp circuit, biased by means of Zener diodes was provided in shunt with the feedback condenser to clamp the integrator output between sweeps. The unusually fast flyback times were obtained by use of a high power, short pulse multivibrator to inject two opposite polarity flyback pulses into each integrating amplifier at two different points to stimulate a fast flyback.

Figure 7 shows the fast "read" sweep waveform from the negative going horizontal channels.

The point of greatest interest is the linearity that was achieved over the large range of sweep speed. This cannot be accurately determined by visual examination of an oscilloscope display of the sweep voltage, but was measured in a more precise fashion by a simple technique involving the use of a simple silicon diode comparator circuit, a precise variable voltage source to bias the comparator, a crystal controlled time mark generator and an oscilloscope. Figures 8 and 9 show the error curves derived from these measurements. The

conclusions from these measurements were that the deviations from linearity did not exceed ± 0.5 per cent of the total sweep amplitude. In the case of the 3 millisecond slow sweep, a linearity of ± 0.1 per cent was almost achieved. In the case of the fast sweep, the linearity was within ± 0.1 per cent over the middle 70 per cent of the sweep, but deviations were considerably larger near the ends.



CALIBRATION:

20 VOLTS/DIVISION,
5 μ SEC./DIVISION

HORIZONTAL OUTPUT

Fig. 7 SWEEP GENERATOR OUTPUT IN THE READ MODE

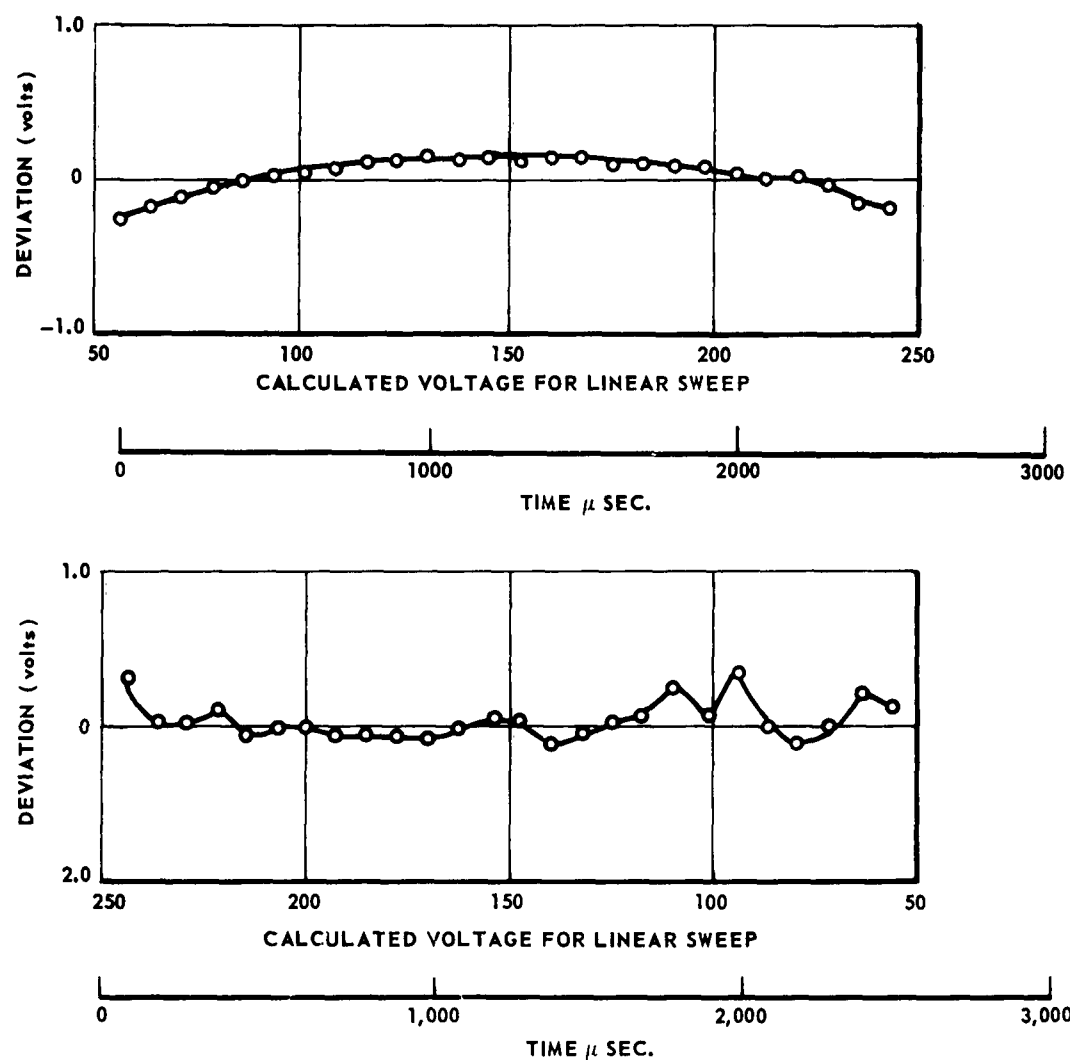


Fig. 8 DEVIATION OF SWEEP VOLTAGE FROM ARBITRARILY CHOSEN
LINEAR SWEEP
(H-WRITE POSITIVE GOING)
(H-WRITE NEGATIVE GOING)

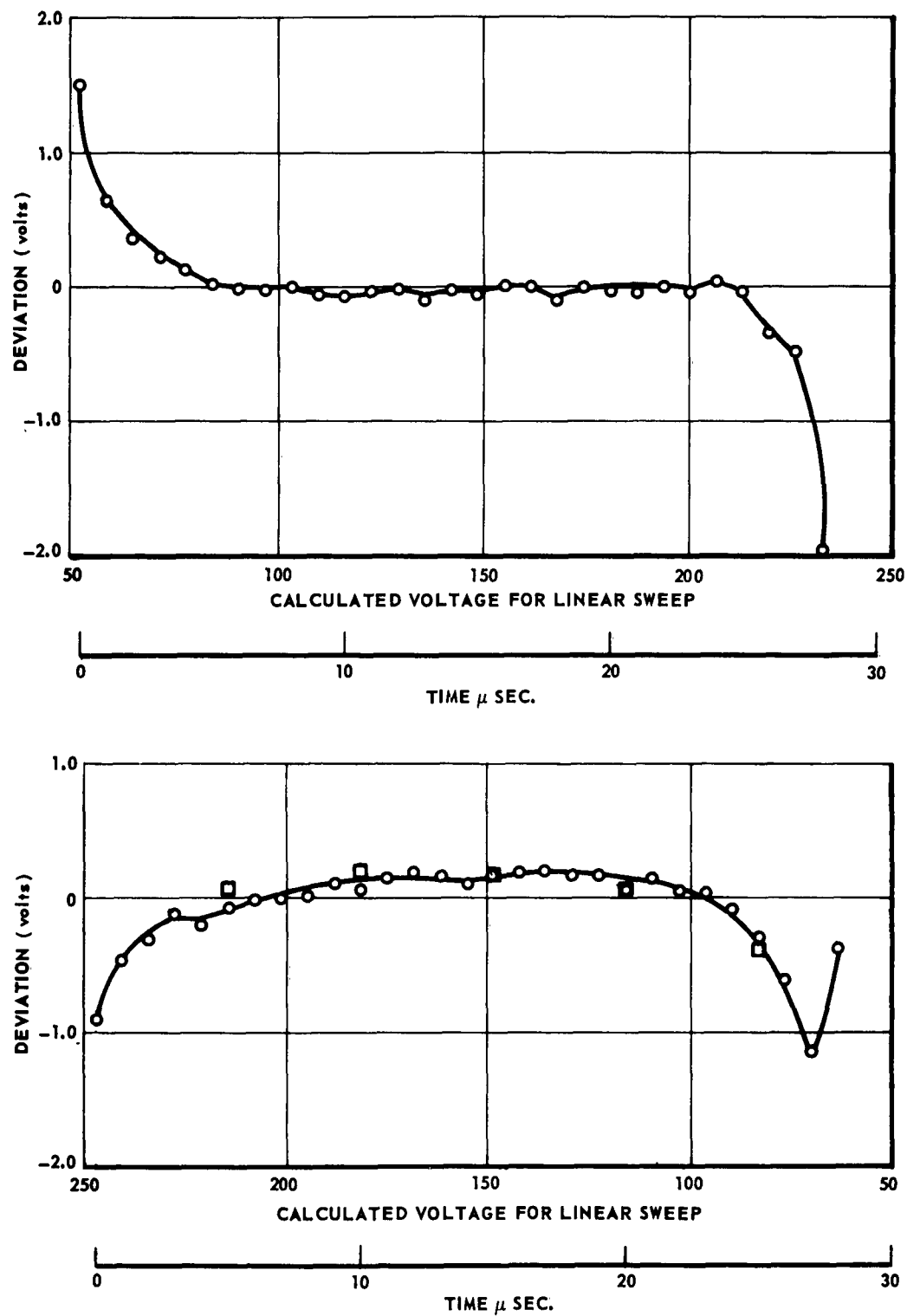


Fig. 9 DEVIATION OF SWEEP VOLTAGE FROM ARBITRARILY CHOSEN
LINEAR SWEEP
(H-READ POSITIVE GOING)
(H-READ NEGATIVE GOING)

The accuracy of these measurements appeared to be limited by noise in the sweep generator output in the case of the fast sweeps and by a small amount of sweep jitter, which was related to sixty cycle pickup in the case of the slow sweeps.

The step waveform, which was specified for the vertical read sweep, was achieved by a minor circuit change, which consisted of coupling a small fraction of the horizontal read voltages into the vertical sweep. The polarity of the coupled signal was such that the slope of the resultant vertical read sweep was reduced to zero during each horizontal sweep. A portion of one of the resultant vertical read sweeps—expanded to show the steps—is shown in Fig. 10.



CALIBRATION:

1.0 VOLT/DIVISION

50 μ SEC./DIVISION

POSITIVE GOING

Fig. 10 EXPANDED VIEW OF A PORTION OF THE VERTICAL
READ OUTPUTS

Storage Tube Unblanking

The unblanking circuits for the storage tube contained some novel features. The unblanking pulse was a-c coupled to the cathode of the storage tube, which operated at 2 kv. In order that a sufficiently long coupling time constant might be obtained with a coupling condenser of reasonable size, a transistor emitter follower circuit was inserted between the coupling condenser and the storage tube cathode. This emitter follower was floating at the same 2 kv potential as the cathode and its collector potential was supplied by Zener diodes located in the high voltage end of the cathode resistor string.

The desirability of unblanking the storage tube electron beam only during the intervals when the beam is being deflected across the storage surface, was based on two considerations. The first had to do with the need to capacitively couple the unblanking pulses into the high voltage circuits of the storage tube cathode and consideration of the short duration of the sweeps compared to the blanked intervals between write and read modes. The second consideration was the need for adequate protection of the storage tube in the event of sweep failure. This protection is provided by initiating unblanking by the fast deflection sweeps.

The requirements called for an unblanking pulse with peak amplitude of 70 to 80 volts with a 0.5 microsecond rise and fall time. This was to be coupled to the high voltage cathode circuits of the storage tube during the intervals of the fast deflection sweeps. At the same time, storage tube bias was to be applied to the cathode of the storage tube. These requirements were met by initiating the unblanking pulse from the differentiated sweep waveform which triggered a gate pulse generator. The negative output of this generator, clamped to ground, is fed to one input of an AND gate. The storage tube bias voltage, supplied by the mode switching section of the Timing Unit, is fed to the second input of the AND gate. Thus, an output unblanking pulse of 0.5 microsecond rise and fall time and having an amplitude determined by the bias level control is coupled into the cathode circuit of the storage tube. In the event of sweep failure, no unblanking pulse is developed and the storage tube is biased off thus providing the necessary protection.

Target Switching

The storage tube requires a means for rapidly switching the backplate voltage from ground potential in the "read" mode to a positive potential in the range of 40 to 60 volts during the "write" mode. In addition, means must be provided to prevent the resulting large transients in the backplate voltage from being coupled into the input of the storage tube output amplifier and driving it so far into saturation that it will take a long time to recover. Since the input of the amplifier is connected directly to the barrier grid, and the barrier grid is coupled to the backplate by a rather large interelectrode capacity (1600 micromicrofarads), the suppression of the

target switching transients is a major problem in the storage tube art and various workers in the field have come up with a variety of rather complicated solutions to the problem.

In the equipment herein described, a comparatively simple solution was arrived at because it was possible to use a relatively long time (several hundred microseconds) to perform the switching. This is in contrast to circuits described in the literature. These are such as might be required in a memory for a high-speed computer where mode switching must be accomplished and the amplifier transients must die out in a very short time of the order of a microsecond. In the present case it was possible to take advantage of the long switching time to operate three cascaded gates in a time sequence such that all three gates attenuate the target switching transient. Each gate produces an additional low level switching transient whenever it is turned on or off. To take care of these transients, the gates are located at points of successively higher signal level. Figure 11 illustrates the arrangement in block diagram form. Mode switching of the storage tube target was accomplished with a single transistor switch, which shorts barrier grid and backplate together during "read." Gate No. 1 is located at the input to the amplifier, gate No. 2 is between the first and second stages of the amplifier, and gate No. 3 is on the output of the amplifier. The gates are turned on in the order 1, 2, 3 and off in the order 3, 2, 1. With this arrangement, each gate attenuates the target switching transient and all gating transients which originate ahead of it in the circuit. The total attenuation from gates 1 and 2 is sufficient so that the amplifier appears to be completely recovered from transient effect by the time the next mode of operation begins. Gate No. 3 was added to further reduce transients to a level below the signal, so there would be no danger of these transients overloading any auxiliary equipment that might be connected to the output amplifier.

In order to obtain the desired effect that each gate attenuate the transient from the preceding gates, it was necessary that at least one short-time constant interstage a-c coupling circuit be located ahead of each gate to insure that the transient passing through the coupling due to a d-c step at the input to the coupling condenser would have died away before the following gate was turned on. Accordingly, RC, high pass, coupling circuits having time constants of the order of 10 microseconds have been interspersed between the gates.

The storage tube input amplifier is of conventional design with 25 db gain between 350 cps and 5 mc. The amplifier

design includes a 6 diode bidirectional gate which is gated on just prior to the storage tube "write-in" interval and is gated off at the end of the interval. Signal rejection during gate cutoff is approximately 40 db. Gating transients during the "write-in" and "read-out" intervals are kept below one per cent of peak signal by switching the gate before unblanking the storage tube beam. Peak-to-peak output of the amplifier is 60 volts.

Storage Tube Output Amplifier

The output amplifier is also of conventional design with a low noise input stage. As used with the WL7225 storage tube output circuits, the amplifier features a gain of either 50 or 65 db between 30 kc and 1 mc which may be selected by means of a selector switch.

Storage Tube Performance

The performance of the storage tube was in agreement with expectations based on the manufacturer's specifications. Resolution was adequate. That is, a pulse could be written in and read out from a single "read-out" line of the 125 line raster without appreciable output from adjacent lines. Uniformity appeared to be within ± 10 per cent over most of the target with slightly greater deviations near the edges.

The noise at the output of the storage tube output amplifier, as estimated by means of a calibrated oscilloscope, was observed to be 0.2 volts peak-to-peak. This is equivalent to 114 microvolts peak-to-peak at the amplifier input (i.e., at

the storage tube target). The theoretical equivalent noise of the input stage as obtained from a standard formula,¹ which applies for the WL7225 storage tube, was found to be 27 microvolts RMS.

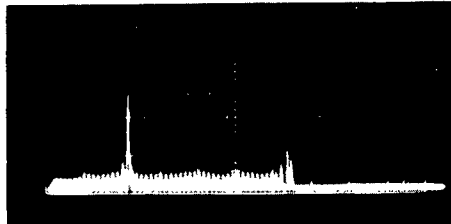
Theoretical calculations based on storage tube and circuit parameters² indicate the expected peak storage tube output signals to be 1.2 millivolts. Performance measurements, based on the same operating parameters assumed in the calculations, resulted in an equivalent peak signal at the storage tube target of 0.9 millivolts.

The ability of the storage tube to store pulse samples of a doppler frequency sine wave and perform time compression by the orthogonal write-read method was checked. This check was accomplished by feeding in randomly timed pulse samples of a 5-kilocycle sine wave from the low-frequency target simulator and passing the storage tube output through a filter tuned to approximately 500 kilocycles. (The ratio of 100 was chosen to match the 100:1 ratio of the "read-to-write" "horizontal sweep speeds.") The output of the filter was detected and displayed on an oscilloscope; Fig. 12 shows the oscilloscope display of the "read" frame interval. Horizontal distance on the display corresponds to target range, and the detected filter output pulse, which results from integration of a train of target pulse, is indicated. The pulse samples were timed to have a fixed delay following each randomly timed vertical "write" sweep trigger pulse.

¹"Reference Data for Radio Engineers," Fourth Edition, ITT Corporation, Stratford Press, 1959, page 421.

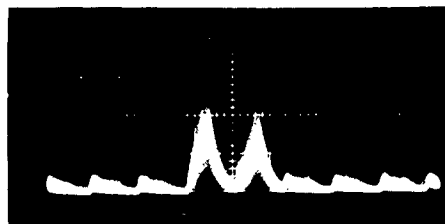
²Formulae and notes of A. S. Jensen and B. Stokes of Westinghouse, Elmira, New York

TARGET SIGNAL



CALIBRATION:
0.1 VOLT/DIVISION, 0.5 M SEC./DIVISION

TARGET ON ONE READ LINE



CALIBRATION:
0.1 VOLT/DIVISION, 50 μ SEC./DIVISION

EXPANDED TIME SCALE, TARGET
BETWEEN TWO READ LINES

Fig. 12 OUTPUT OF TIME-COMPRESSED DOPPLER FILTER AND
DETECTOR CIRCUIT DURING THE READ FRAME INTERVAL
(TARGET SIGNAL FROM SIMULATOR)

As a result, a horizontal line of pulses such as might be obtained from a target, was stored on a single "read-out" line. When this line of pulses was read out, the integration and detection processes in the filter detector circuit converted it to the single pulse shown on the display. Figure 12 (upper) shows the detected filter output with the delay adjusted to position the pulses accurately on a single "read-out" line. Figure 12 (lower) shows the output when the delay was changed slightly so that the pulses were written in half way between the read-out lines. In this case, an output of reduced amplitude was obtained from the two "read-out" lines, and; consequently, two adjacent pulses appear on the display.

When the 5 kc input signal generator being sampled was detuned in either direction, the output pulse from the 500 kc output filter decreased. This indicates that time compression by the expected factor of 100:1 was, in fact, achieved.

Master Timing and Mode Switching Unit

The Master Timing and Mode Switching Unit is designed to supply synchronization, trigger and gating pulses to the entire Range and Spectrum Analyzer System. The basic timing accuracy is derived from a one mc oven-controlled crystal oscillator.

Figure 13 is a block diagram showing the system timing unit interconnections.

Considerable versatility is designed into the timing unit by utilizing preset counters and digital logic circuitry in both the "write-in" and "read-out" modes. The circuitry is interconnected in such a way as to form a closed-loop path

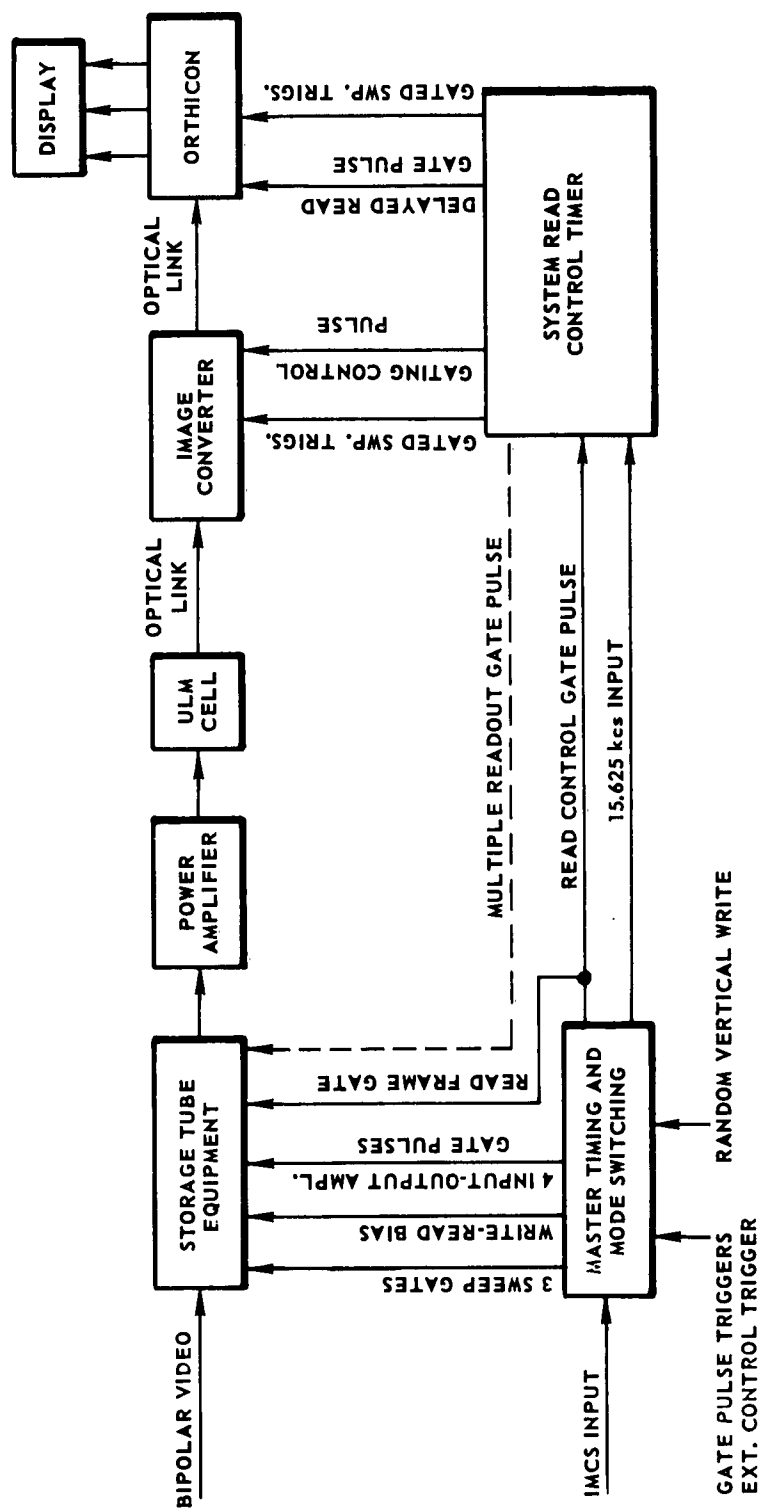


Fig. 13 BLOCK DIAGRAM SHOWING SYSTEM TIMING INTERCONNECTIONS

for switching. As a result, the Analyzer System can cycle continuously to provide alternate "write" and "read" modes of operation without external control. However, provision is also made for external control of the system in the event it becomes desirable to "slave" the system to external equipment. This latter mode of system operation permits a spectrum analysis to be made of a single cycle of operation or of repeated cycles of operation at a random rate.

By proper positioning of selector switches, the system timing will automatically permit a single "write-in" frame of information to the storage tube followed by either one or more storage tube "read-out" frames. The stored information in the first of the storage tube "read-out" frames is coupled into the ULM-Cell during which time the image converter is gated on and the image orthicon will be gated off. After a preset delay corresponding to a storage tube "read-out" frame, the image converter will be gated off and the image orthicon will be gated on to read out the spectrum information. During the time allotted for the image orthicon readout the storage tube will continue to cycle through a number of "read-out" frames. These additional storage tube read-out cycles permit a more complete erasure of the storage surface in preparation for new information. At the end of the system "read-out" interval, the timer automatically reverts to the "write-in" mode. If internal control of the timer is used, the equipment recycles; however, if the timer is controlled by external triggers, the equipment locks in the "write-in" mode with the storage tube beam blanked off until the arrival of the next external trigger which starts the new cycle of operation.

Effective switching of the storage tube bias level over an adjustable range of 70 volts, input and output amplifier gating, write and read vertical and horizontal sweep-gating, storage tube unblanking and storage target gating are provided by the mode switching section of the Timing Unit. Accurate timing and pulse shaping is provided to minimize transients at the storage tube output.

Ultrasonic Cell

The ultrasonic spectrum analyzer is based upon the ultrasonic light modulator cell in which sonic waves in a liquid are used to diffract light waves.

The basic system is shown in Fig. 14. The cell is filled with liquid and contains a piezo crystal at one end and a sponge rubber or metal wool absorber at the other end. If a sinusoidal voltage is applied to the crystal, traveling pressure waves are produced in the liquid. Since the index of refraction varies with pressure, we obtain a sinusoidal variation of refractive index.

The source of light is a slit and is also monochromatic with wavelength λ . The light is collimated by the first lens, passes through the cell, and is focussed onto the image plane by a lens of focal length F . If no signal is applied to the crystal, an image of the slit is obtained on the optical axis. If a sinusoidal voltage is applied to the crystal, the liquid in the cell acts as a phase grating due to the sinusoidal variation in refractive index. Just as in the case of an optical transmission grating, we find lines in the image plane at an angle θ from the optical axis, where

$$\sin \theta = \frac{m\lambda}{\Lambda}$$

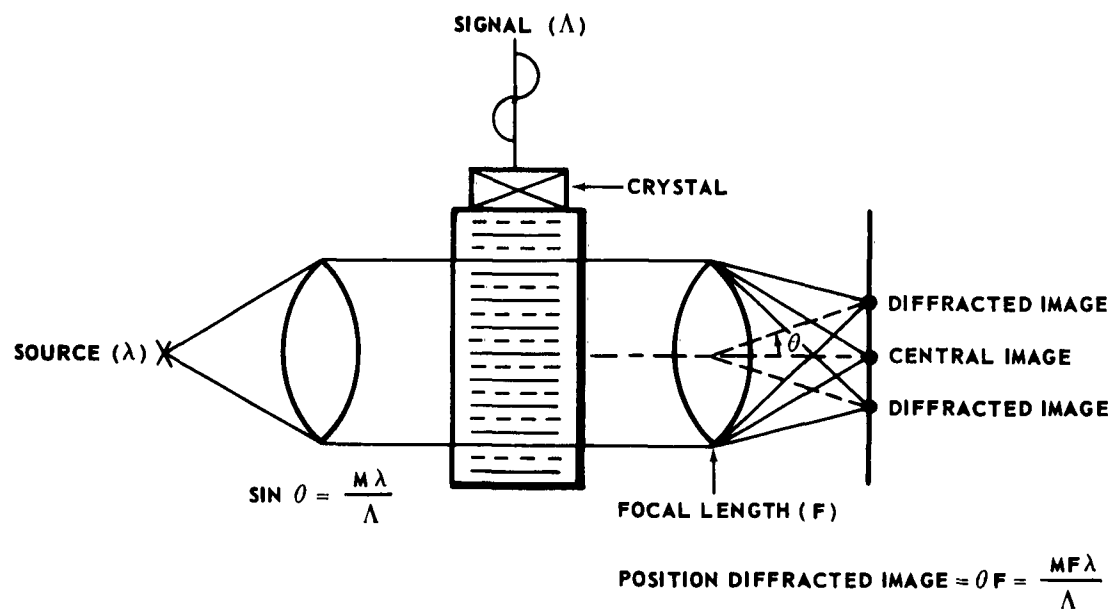


Fig. 14 ULTRASONIC LIGHT MODULATOR

Here Λ is the sonic wavelength and m takes on values of ± 1 , ± 2 , etc., representing various orders.

The intensity of an m 'th order line is proportional to the square of the m 'th order Bessel function whose argument is proportional to the applied voltage and crystal diameter and inversely proportional to the sonic wavelength. When we confine ourselves to the first order only and make a first term approximation, we conclude that the line intensity increases with crystal diameter and applied voltage and inversely with wavelength. The location of this line is proportional to the applied frequency. We thus have the elements of a spectrum analyzer.

A number of experiments were conducted to verify that the cell is indeed a spectrum analyzer. In one experiment, two sine waves were mixed and applied to the crystal. The two frequencies selected were separated by 1 mc to stay within the crystal pass band. It can be shown theoretically that the resulting lines should correspond to sums and differences of integral multiples (or orders) of the individual frequencies. The intensities are now proportional to products of the squares of Bessel functions. In our experiment, we were able to see 37 lines on one side of the central image. The frequencies were identified by measuring separations with a traveling microscope.

In the second experiment, we applied a train of rectangular pulses whose frequency spectrum is a series of harmonics separated by $1/T$ and whose amplitude varies as $\frac{\sin x}{x}$.

The pulse width was chosen so that the second lobe of the $\frac{\sin x}{x}$ curve would fall in the vicinity of the crystal's resonance. Figure 15 shows the results. The intense center line is the central undiffracted line. All intensities appear

to roughly follow the variation of harmonic amplitudes modified by the crystal response.

A final test was made with a bipolar video signal simulating the storage tube output. This signal was mixed with a 15.25 mc carrier in a balanced modulator. The resulting sidebands were amplified and applied to the crystal. Since the crystal resonant frequency was 14.75 mc, the lower sideband was placed near the crystal's peak thus giving maximum intensity. Results are shown in Fig. 16. The last two lines show the effect of adding noise. Here the carrier could not be balanced out.

Light Source

A number of light sources were investigated for brightness within a narrow spectral region. The green line at 5461 Å from a mercury arc was selected. The lamp finally chosen was the Osram HBO/109 whose surface brightness measured 8.2 watt/cm²/Å, and which consumes 100 watts. Narrow band interference filters must be used as the spectral lines are much too wide for this application.

Optics and Photometry

The basic optical system is shown in Fig. 17. The light source B is condensed by condenser F₁ and F₂ on the slit; A is a narrow band interference filter. The light passing through the slit is collimated by F₃, passes through the ULM cell and focussed by the focussing lens F₄ into the converter cathode. A detailed analysis of the optics, photometry, converter and orthicon signal level problem is given

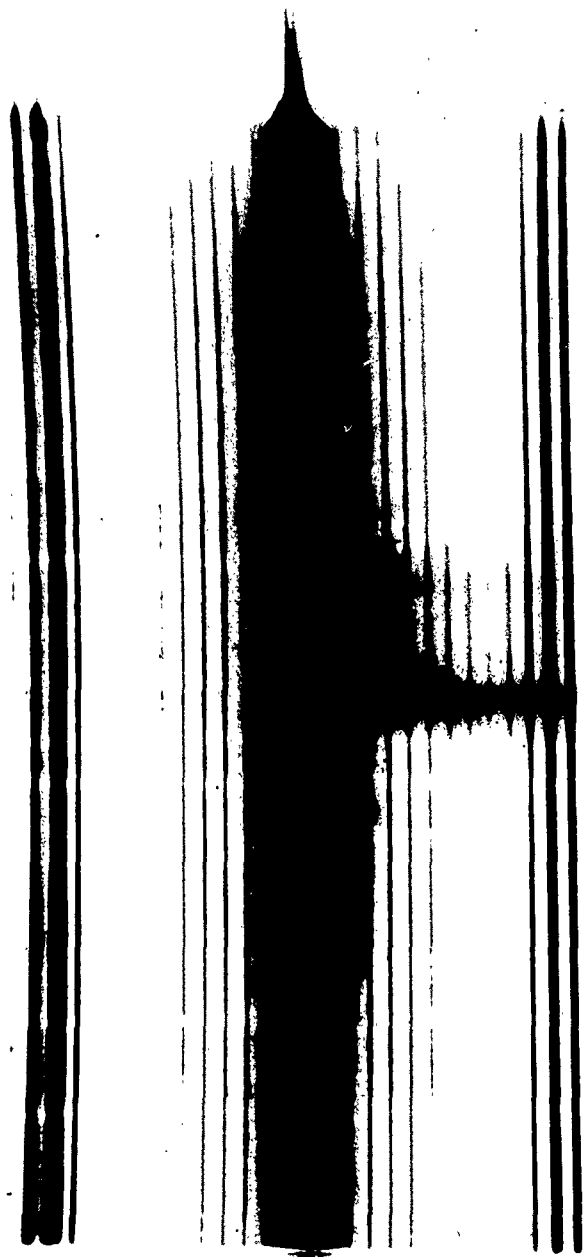


Fig. 15 SPECTRAL COMPONENTS OF A TRAIN OF SQUARE PULSES --
ANALYSIS BY ULTRASONIC CELL

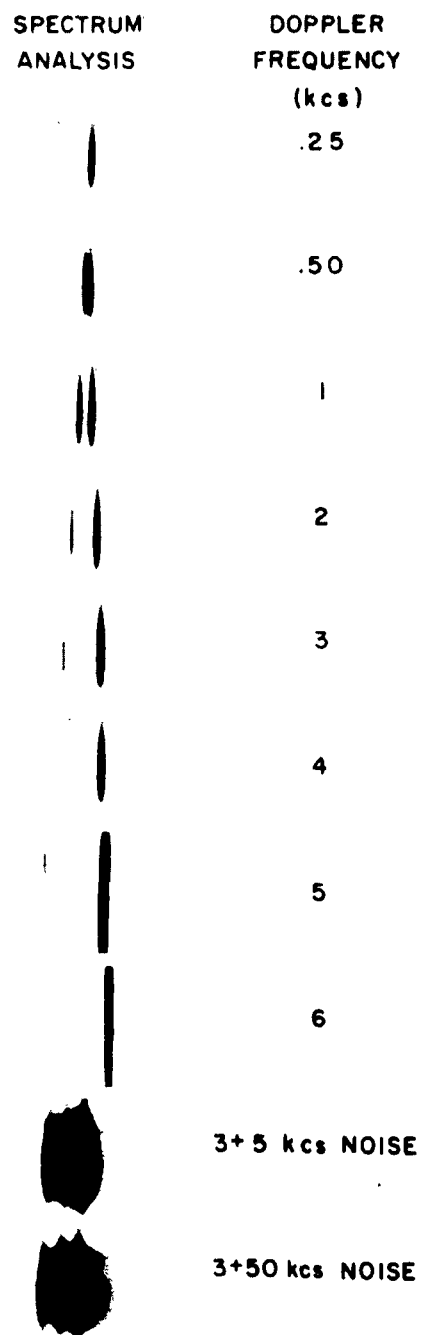
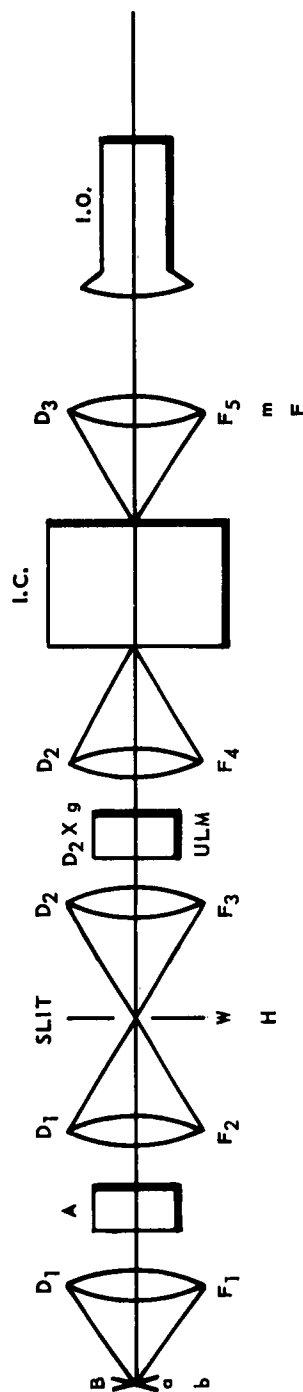


Fig. 16 14.75 MC ULTRASONIC LIGHT MODULATOR MAKING SPECTRUM
 ANALYSIS OF RANDOM BIPOLAR VIDEO PULSES



- B = LIGHT SOURCE OF WIDTH a , AND HEIGHT b , BRIGHTNESS B
 F_1 = FIRST CONDENSER LENS OF FOCAL LENGTH F_1 , DIAM D_1
 F_2 = SECOND CONDENSER LENS OF FOCAL LENGTH F_2 , DIAM D_1
 F_3 = COLLIMATING LENS OF FOCAL LENGTH F_3 , DIAM D_2
 F_4 = FOCUSING LENS OF FOCAL LENGTH F_4 , DIAM D_2
 A = OPTICAL FILTER WHICH ISOLATES A BANDWIDTH $\Delta\lambda$ AT λ
 λ IS THE WAVELENGTH OF THE LIGHT USED.
 SLIT = SLIT OF WIDTH w , HEIGHT H
 ULM = ULTRASONIC LIGHT MODULATOR CELL
 IC = IMAGE CONVERTER
 IO = IMAGE ORTHICON
 F_5 = LENS OF FOCAL LENGTH F_5 , DIAM D_3 , f/F , AND MAGNIFICATION m

Fig. 17 OPTICAL SYSTEM USED WITH ULTRASONIC CELL, IMAGE CONVERTER, AND IMAGE ORTHICON

in "Optics and Photometry of the ULM," Applied Physics Laboratory, CF 2846.

The width of the slit image when focussed on the converter is $(F_4/F_3)W$. Due to diffraction in the ULM cell, the smallest slit image is $2\lambda F_4/D_2$. For optimum design

$$(F_4/F_3) W = 2\lambda F_4/D_2.$$

The resolution of the cell is $f/\Delta f = D_2/\Lambda = D_2 f/v$, where v is the sonic velocity, Δf the separation of two lines which can just be discerned separately, and Λ is the sonic wavelength in the cell fluid. Since the dispersion of the cell is $\lambda F_4/v$, we have for the filter bandwidth $(\Delta\lambda)$

$$\Delta\lambda f F_4/v = 2\lambda F_4/D_2$$

$$\Delta\lambda = 2\lambda v f/D_2$$

The required cell length is found from the condition that the resolution in the cell is 30 kc (300 x 100), so $D_2 = v/30 \text{ kc} = 150 \times 10^3 / 30 \times 10^3 = 5 \text{ cm}$. A 5 cm cell at 20 mc was selected since it was easily available. The liquid used was water plus 10 per cent ethyl alcohol to minimize the variation of the sonic velocity with temperature. The value of v is $150 \times 10^3 \text{ cm/sec}$.

ULM Cell Driving Amplifier

The driving amplifier accepts the bipolar video pulses from the storage tube. This signal is applied to a linear balanced modulator which shifts the frequency components up to the 20 mc region, which is the operating frequency for the final crystal used. Both sidebands are carried with one centered at the crystal's resonant frequency.

The remainder of the amplifier is devoted to relatively wideband amplification. A final output of 950 volts peak-to-peak with a 4 mc bandwidth is obtainable. The frequency response was intentionally made wider than was necessary for the particular parameters in this experimental system so that the cell's ability to extract a doppler from noise could be demonstrated.

The output stage is a 4X-250 transmitting tube operated as a class AB radio frequency linear amplifier, except that a very low Q tuned plate load is used. Such an arrangement can give a fairly wide bandwidth and still produce good attenuation for harmonics of the carrier.

The quartz crystal's capacitance was tuned out and shunted with a 1000 ohm load resistor. This load resistor preserves bandwidth and gives a near optimum load for the output tube.

Image Converter

The image converter, as mentioned previously, is used to gate the spectrum analyzer on when the diffraction cell is filled with pulses from the storage tube and to deflect the images of successive range elements to contiguous positions to build up a range scale.

The only suitable tube known to be in production at the time we assembled the system was the RCA - C73435B. This tube has an S-11 photocathode and a P-11 phosphor. It operates at 15 kv, may be gated on and off with 300 volt pulses, and allows electrostatic deflection at 1100 to 1200 volts per inch.

As finally used, the gating grid was biased off at -130 volts. When the storage tube output was passing through the ultrasonic cell, the gating grid was pulsed on to +200 volts. The optimum on time was determined experimentally to be about 8-microseconds, although this value was not critical. However, it was important that the on period symmetrically encompass the instant when the cell is completely filled with pulses (at the completion of the storage tube readout). Pains were taken to achieve a gating pulse rise time of less than 1-microsecond since this tube defocusses while in a partial on condition.

A range display is developed by applying to the deflection plates a staircase in step with the storage tube readout. A staircase is desired, rather than a sawtooth, to avoid motion during the writing of a spot on the screen which would cause a degradation of resolution. Chopper-stabilized amplifiers are used in the deflection circuits to obtain precision.

One unfortunate feature of the image converter is the considerable rise time for the phosphor image. For the 8- or 10-microseconds on time used, the phosphor failed to reach equilibrium intensity by a factor of five, resulting in a serious loss of the signal.

III. ACQUISITION SYSTEM PERFORMANCE

A prototype acquisition system was assembled as shown in Fig. 18. The ULM cell was 5 cm long with a 20 mc crystal of 11.8 mm free diameter. The cylindrical lens next to the converter was used to compress the image height, the other cylindrical lens being used to increase the horizontal dispersion. The converter phosphor was viewed with a 20-power microscope. The storage tube was set up to use 50 range elements with a 10 microsecond vertical "write" sweep.

With this system the converter range deflection was set so that the range elements were individually resolvable. The image was bright enough so that the spot of light corresponding to the doppler frequency was easily visible. Figure 19 is a photograph of the result.

By varying the simulated doppler frequency in the simulator, the light spot was caused to move along the doppler scale as predicted. By varying the sampling delay, the target range could be varied, and the position of the light spot was caused to move along the range axis as expected.

Figure 19a is a range-doppler display with no added noise, while Figure 19b is the result obtained when noise is added to simulate jamming. The signal power per resolution element was four times the noise power.

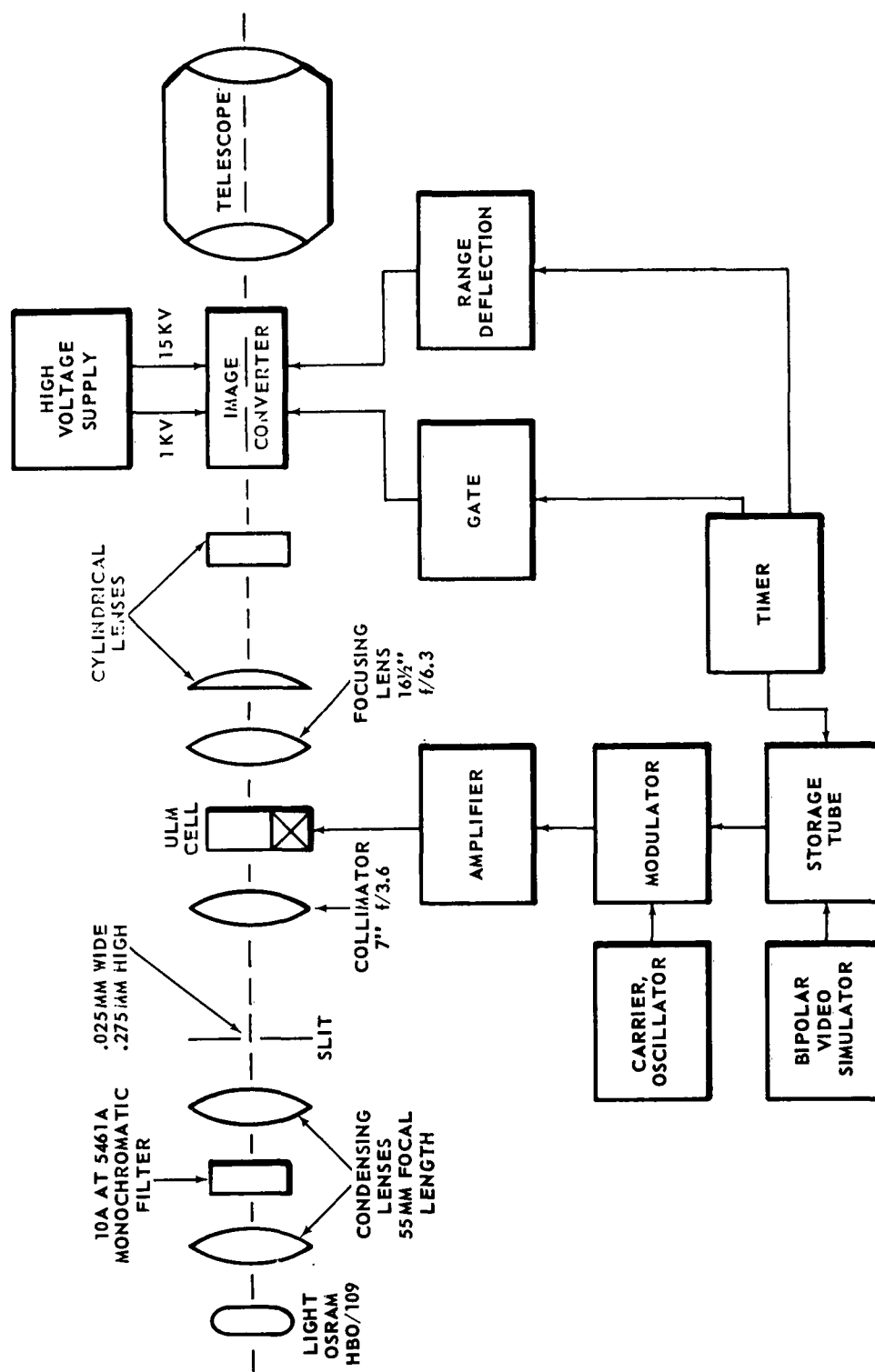


Fig. 18 PROTOTYPE ACQUISITION SYSTEM

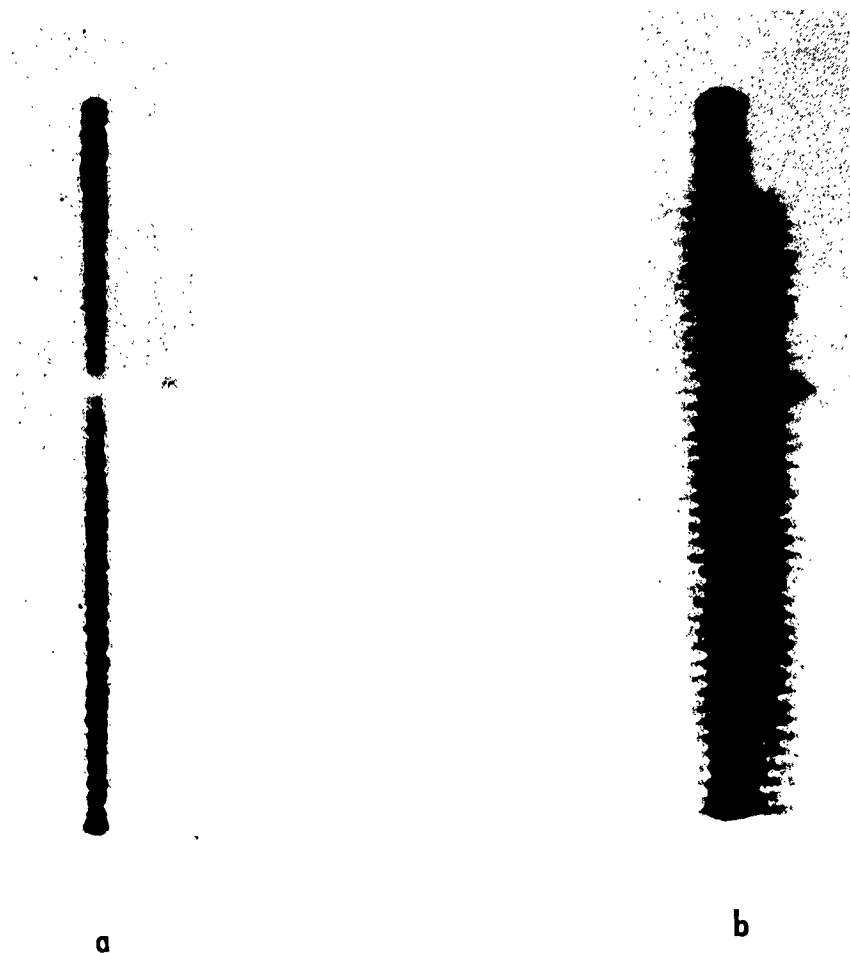


Fig. 19 RANGE-DOPPLER DISPLAY WITH AND WITHOUT ADDING
JAMMING NOISE

This report is one of the CM series which consists of technical papers or extensive progress reports that are characterized by an intensive treatment of the subject matter. CM reports have received official Laboratory review to substantiate the validity of their technical content and to establish suitability for distribution outside of Section T to qualified personnel in the pertinent technical fields.

In addition to internal (Section T) distribution, the initial distribution of this document has been made in accordance with Guided Missile Technical Information Distribution List MML 200/23 List No. 23, dated 3 April 1961.